

# **The Rab-interacting lysosomal protein (RILP) regulates vacuolar ATPase acting on the V1G1 subunit**

**Maria De Luca<sup>1</sup>, Laura Cogli<sup>1</sup>, Cinzia Progida<sup>1,3</sup>,  
Veronica Nisi<sup>1</sup>, Roberta Pascolutti<sup>2</sup>, Sara Sigismund<sup>2</sup>,  
Pier Paolo Di Fiore<sup>2</sup>, and Cecilia Bucci<sup>1,\*</sup>**

<sup>1</sup>Department of Biological and Environmental Sciences and Technologies, (DiSTeBA) University of Salento, Via Provinciale Monteroni 165, 73100 Lecce, Italy

<sup>2</sup>IFOM, Fondazione Istituto FIRC di Oncologia Molecolare, Via Adamello 16, 20139, Milan, Italy.

\* Corresponding author. Cecilia Bucci, Dipartimento di Scienze e Tecnologie Biologiche ed Ambientali, Università del Salento, Via Provinciale Monteroni 165, 73100 Lecce, Italy. Tel.: +39 0832 298900; Fax: +39 0832 298626; E-mail: [cecilia.bucci@unisalento.it](mailto:cecilia.bucci@unisalento.it)

<sup>3</sup>Present address: Centre for Immune Regulation, Department of Molecular Biosciences, University of Oslo, 0316 Oslo, Norway

Running Title: RILP regulates V-ATPase

## Summary

RILP is a downstream effector of the Rab7 GTPase. GTP-bound Rab7 recruits RILP on endosomal membranes and, together, they control late endocytic traffic, phagosome and autophagosome maturation and are responsible for signaling receptor degradation. We have identified, using different approaches, the V1G1 subunit of the vacuolar ATPase (V-ATPase) as a RILP interacting protein. V1G1 is a component of the peripheral stalk and it is fundamental for correct V-ATPase assembly. We established that RILP regulates the recruitment of V1G1 subunit to late endosomal/lysosomal membranes but also controls V1G1 stability. Indeed, we demonstrated that V1G1 is ubiquitinated and that RILP is responsible for proteasomal degradation of V1G1. Furthermore, we demonstrated that alterations of V1G1 expression levels impair V-ATPase activity. Thus, our data demonstrate for the first time that RILP regulates the activity of the V-ATPase through the interaction with V1G1. Given the importance of V-ATPase in several cellular processes and human diseases, these data suggest that modulation of RILP activity could be used to control V-ATPase function.

Key words: RILP; vacuolar ATPase; Rab7; V1G1; ubiquitin

## Introduction

Vacuolar-type  $H^+$  ATPases (V-ATPases) are large multi-subunit complexes that control acidity of intracellular compartments and are also responsible for proton transport across the plasma membrane and thus for acidification of the extracellular environment (Forgac, 2007; Sun-Wada et al., 2004; Toei et al., 2010). They are proton pumps conserved in all eukaryotes, and organized into two-domains that constitute a rotary machine (Cipriano et al., 2008; Kane, 2006; Kane and Smardon, 2003). V0 is the integral transmembrane domain responsible for proton translocation, while V1 is the peripheral domain located in the cytoplasmic site of the membrane and it is responsible for ATP hydrolysis providing energy to pump the protons (Cipriano et al., 2008; Kane, 2006; Kane and Smardon, 2003). Accurate control of pH of intracellular organelles and extracellular milieu is fundamental for many cellular processes as, for instance, processing and degradation of macromolecules in secretory and digestive compartments, coupled transport of small molecules as neurotransmitters, but also sperm maturation and osteoclast function. Defects in acidification have been recently recognized as an important cause of several severe human diseases as renal tubule acidosis, osteopetrosis, defects in sperm maturation and diabetes (Casey et al., 2010; Marshansky and Futai, 2008). In addition, V-ATPase activity regulates membrane fusion, early to late endosomal trafficking, and neurosecretion (El Far and Seagar, 2011; Hurtado-Lorenzo et al., 2006; Qiu, 2012). Importantly, V-ATPases contribute to invasive properties of tumor cells (Forgac, 2007; Sennoune et al., 2004b). In tumor cells V-ATPases are targeted to the plasma membrane and acidify the extracellular environment, activating lysosomal enzymes that are responsible for the degradation of extracellular matrix. Thus V-ATPases are directly involved in invasiveness, also of endothelial cells during angiogenesis, and are now considered a very promising target against metastasis (Forgac, 2007).

The reversible dissociation of the complex into the V1 and V0 domain represent a fundamental control mechanism of V-ATPase function that is responsible for varying rates of pumping (Forgac, 2007). However, also reversible dissociation of single subunits has been reported to regulate V-ATPase activity (Qi et al., 2007). A complex named RAVE regulates pumps assembly (Smardon et al., 2002). In addition, also extracellular pH regulates strongly V-ATPase activity and assembly (Diakov and Kane, 2010).

RILP (Rab Interacting Lysosomal Protein) is an effector of the small GTPase Rab7 (Cantalupo et al., 2001; Bucci et al. 1988; Chavrier et al. 1990). Rab proteins localize to the cytosolic side of intracellular organelles and regulate membrane traffic (Aloisi and Bucci, 2013; Bucci and Chiariello, 2006; Stenmark, 2009). Rab7, in its active GTP-bound form, recruits RILP on membrane and together they control trafficking to late endosomes and lysosomes in the endocytic route (Bucci et al., 2000; Cantalupo et al., 2001; Jordens et al., 2001). Furthermore, RILP is involved in the biogenesis of multivesicular bodies (Progida et al., 2007; Progida et al., 2006).

Using the two-hybrid system, we have isolated the V1G1 subunit of V-ATPase as a RILP interacting protein. Our data indicate that RILP, through its direct interaction with V1G1, regulates the function of V-ATPase. Thus, we have discovered a new regulatory mechanism of V-ATPase function, and, given the involvement of V-ATPase in several human diseases, these data suggest that RILP could become a useful target for development of effective therapeutical means.

## Results

### **RILP interacts with the V1G1 subunit of the V-ATPase**

A yeast two-hybrid screen was used to identify proteins that interact with RILP. A Gal4-binding domain/RILP fusion construct was made in pGBKT7 vector and used in the screen to identify putative interactors. The construct was used to screen a liver cDNA library encoding proteins as C-terminal fusions with the transcriptional activation domain of Gal4 in the pACT2 vector. From  $1,3 \times 10^6$  primary transformants, 27 were His<sup>+</sup>LacZ<sup>+</sup> and were encoding true positives that did not activate transcription in the presence of a non-specific test bait. Seven transformants encoded the entire V1G1 subunit of the vacuolar ATPase. The interaction was revealed by the growth of yeast cells expressing RILP and V1G1 on synthetic medium lacking histidine and adenine. In the two-hybrid system the interaction was specific as the yeasts expressing V1G1 together with Rab7 were not able to grow without histidine, or without histidine and adenine (Fig. S1A). These results were confirmed using the other reporter gene,  $\beta$ -galactosidase (Fig. S1B). Using a  $\beta$ -galactosidase quantitative liquid assay, we confirmed the interaction between RILP and V1G1 and established, using previously described RILP deletion mutant constructs (Colucci et al., 2005a), that V1G1 binds to the N-terminal half of RILP (Fig. S1).

To confirm the results obtained with the two-hybrid screen we investigated whether the two proteins were able to co-immunoprecipitate. HeLa cells were transfected with constructs expressing HA-tagged RILP, V1G1, both or non transfected (NT) and immunoprecipitation was performed using an anti-HA resin. Immunoprecipitates of HA-tagged RILP contained the V1G1 subunit of V-ATPase therefore confirming the interaction (Fig. 1A). In addition, by overexpressing V1G1, RILP, RILPC33 and RILP $\Delta$ C2 we established that V1G1 could be immunoprecipitated also by RILP $\Delta$ C2 but not by RILPC33 (Fig. 1B), thus confirming the data obtained with the two-hybrid system indicating that V1G1 binds to the N-terminal half of RILP (Fig. S1). In order to verify the physiological significance of the interaction we also demonstrated co-immunoprecipitation of RILP and V1G1 endogenous proteins using a crosslink immunoprecipitation kit as described in Material and Methods (Fig. 1C).

Subsequently, to check if the interaction was direct, we purified bacterially expressed GST, GST-tagged RILP, GST-tagged RILPC33 and His-tagged V1G1. Glutathione resin alone or bound to GST, GST-RILP or GST-RILPC33 was incubated with His-tagged V1G1. V1G1 subunit was specifically bound only to GST-tagged RILP demonstrating a direct interaction between V1G1 and RILP (Fig. 1D).

Altogether, these results demonstrate that RILP is able to interact physiologically and directly with the V1G1 subunit of the vacuolar ATPase.

### **RILP interacts simultaneously with V1G1 and p150<sup>Glued</sup>**

RILP is able also to interact directly with the C-terminal domain of the dynactin projecting arm p150<sup>Glued</sup>, controlling transport of Rab7-positive organelles toward the cell center (Cantalupo et al., 2001; Jordens et al., 2011; Johansson et al., 2007; Harrison et al., 2003). Since acidification of endosomes correlates with their translocation toward the microtubule organizing center, we investigated whether the interactions of RILP with p150<sup>Glued</sup> and V1G1 are mutually exclusive. Using purified His-V1G1 bound to Ni-NTA resin we were able to pull down FLAG-p150<sup>Glued</sup> from lysates of transfected HeLa cells only in the presence of purified GST-RILP (Fig. 1E).

These data indicate that RILP can bind at the same time V1G1 and p150<sup>Glued</sup>.

### **RILP expression levels affect V1G1 abundance**

To investigate the role of this interaction we decided to analyze whether modulation of RILP expression levels affected V1G1 abundance. Interestingly, upon RILP overexpression the total amount of the V1G1 subunit in HeLa cells was reduced (Fig. 2A). In contrast, in RILP-silenced cells the amount of V1G1 was strongly increased (Fig. 2B). Importantly, RILP overexpression or silencing did not affect V1C1 and V0D1, two other V-ATPase subunits (Fig. 2A, B) indicating that RILP regulates specifically this subunit. Notably, expression of RILP $\Delta$ C2 or RILP $\Delta$ C33 did not affect V1G1 abundance (Fig. 2C) suggesting that only the entire protein is able to act on V1G1 protein abundance. Furthermore, overexpression of HA-tagged RILP was able to partially rescue the effect on V1G1 abundance in RILP-silenced cells thus excluding off-target effects (Fig. 2D).

To establish if the changes observed on V1G1 protein amount were a consequence of mRNA abundance, we checked V1G1 mRNA expression using real time PCR (Fig. 2G). As expected in cells transfected with HA-RILP, RILP mRNA was increased while in RILP-silenced cells, RILP mRNA decreased (Fig. 2E, F). Interestingly, we found that the amount of V1G1 mRNA upon RILP overexpression is slightly increased while it is decreased upon RILP silencing (Fig. 2G). Thus mRNA expression seems to be altered in order to try to counteract the effects on V1G1 protein amount caused by RILP overexpression or silencing.

### **RILP induces proteasomal degradation of V1G1**

As we established that RILP expression levels regulate V1G1 amount, we then decided to investigate whether RILP was responsible for V1G1 proteasomal degradation. We overexpressed RILP and treated cells with the proteasome inhibitor MG132. In these conditions the endogenous V1G1 protein level did not decrease suggesting that RILP regulates proteasomal degradation of V1G1 (Fig. 2H). We then decided to investigate if V1G1 was ubiquitinated. We expressed HA-V1G1 in HeLa cells in presence and absence of the proteasomal inhibitor MG132 and in presence or absence of RILP overexpression. Lysates of cells were then immunoprecipitated with anti-HA resin and subjected to Western blot analysis using an anti-ubiquitin antibody. Ubiquitination of V1G1 was present in all samples where HA-V1G1 was expressed and immunoprecipitated, but was increased in the presence of MG132 suggesting a strong regulation of V1G1 mediated by the proteasome. The V1G1 protein amount

decreases upon RILP overexpression while treatment with MG132 partially rescues V1G1 levels and strongly increases ubiquitination forms of V1G1. Hence, taking into consideration V1G1 levels, RILP overexpression induces V1G1 ubiquitination (Fig. 2I).

### **RILP recruits V1G1 on late endosomal/lysosomal membranes**

We then analyzed if RILP is responsible for recruitment of V1G1 on membranes. We treated cells with MG132 in order to prevent V1G1 ubiquitin-dependent proteasomal degradation induced by RILP and we looked at cytosolic and membrane distribution of endogenous V1G1 in control cells and in cells overexpressing RILP. As loading controls we used GAPDH, a cytosolic protein, and V0D1, a membrane subunit of V-ATPase. Expression of HA-RILP did not change the membrane/cytosol distribution of GAPDH and V0D1. The analysis of the distribution of V1G1 showed that the amount of membrane-associated V1G1 increased upon RILP overexpression while the amount of cytosolic V1G1 decreased (Fig. 3A). Indeed, RILP overexpression increased membrane localization of V1G1 of about 30% while cytosolic V1G1 diminished to 85% compared to control (Fig. 3B). These data demonstrate that, upon RILP overexpression, V1G1 membrane localization increases and suggest that RILP could recruit V1G1 on endosomal and/or lysosomal membranes.

Having showed that RILP controls V1G1 amount and recruitment on membranes, we decided to investigate whether V1G1 binds to RILP when is in complex with other V-ATPase subunits. We immunoprecipitated, using an anti-HA resin, HA-tagged RILP from lysates of HeLa cells expressing HA-tagged RILP and endogenous or overexpressed V1G1. In both immunoprecipitates we observed the presence not only of V1G1 but also of V1C1 and V0D1, two other V-ATPase subunits (Fig 3C). Larger amounts of co-immunoprecipitated V1G1, obtained when V1G1 was overexpressed, led to increased co-immunoprecipitation of the other two subunits (Fig. 3C). These data suggest that V1G1 interacts with RILP alone or complexed with the other subunits thus suggesting that RILP could be important for controlling assembly of the entire pump at the endosomal membranes by recruiting V1G1.

We also analyzed by confocal immunofluorescence analysis the intracellular localization of V1G1 upon RILP overexpression. As commercially available antibodies against the V1G1 subunit of V-ATPase do not work by

immunofluorescence we looked at localization of overexpressed HA-tagged V1G1 subunit. As expected, V1G1 was partially colocalizing with Lamp1 on late endosomal and lysosomal structures (Fig. 4). Expression of RILP caused clustering of late endosomal and lysosomal structures, as previously reported (Cantalupo et al., 2001; Colucci et al., 2005b) and HA-tagged V1G1 was localized onto the clustered structures generated and marked by GFP-RILP (Fig. 4A). Interestingly, upon RILP overexpression, the colocalization percentage of V1G1 with Lamp1 is increased (Fig. 4A, B). In contrast, expression of RILP-C33, the deletion mutant containing only the C-terminal half of RILP that does not interact with V1G1, decreases colocalization with Lamp1 (Fig. 4A, B). These data suggest that localization of V1G1 on late endosomal/lysosomal membrane is regulated by RILP. Furthermore HA-tagged V1G1 partially co-localized with RILP on late endosomal/lysosomal structures labelled with Lamp1 while very little co-localization was detected with RILPC33 (Fig. 4A). Quantification data (Fig. 4C) indicate that less than 10% of co-localization was found between HA-V1G1 and RILPC33, thus confirming the interaction data.

In addition, we analyzed the effects of RILP silencing on HA-tagged V1G1 localization (Fig. 5). Interestingly, in RILP-depleted cells (RILPi) the colocalization of HA-tagged V1G1 with Lamp1 decreased, thus confirming the role of RILP in recruiting V1G1 on late endosomal and lysosomal membranes (Fig. 5). In addition, upon RILP silencing, the colocalization of HA-tagged V1G1 with giantin, a marker of the Golgi complex, strongly increased indicating that, in the absence of RILP, V1G1 localizes mainly to other compartments (Fig. 5).

Altogether these data indicate that RILP recruits V1G1 on late endosomal and lysosomal membranes and suggest that RILP could be important for the assembly of the pump on these organelles.

### **RILP is in complex with V1G1 together with Rab7**

RILP is a Rab7 effector protein and, thus, in order to investigate whether Rab7 is also involved in the regulation of V1G1 we transiently overexpressed or silenced Rab7 and looked at V1G1 abundance (Fig. 6A, B). Interestingly, Rab7 overexpression didn't affect V1G1 abundance while Rab7 silencing caused a strong decrease in the amount of V1G1 (Fig. 6A, B). Furthermore, the decrease of V1G1 amount caused by RILP overexpression was counteracted by Rab7 overexpression (Fig. 6C) thus suggesting that when RILP binds Rab7 does not induce V1G1 degradation.



In order to further investigate the role of Rab7 in the interaction between RILP and V1G1 we expressed in HeLa cells HA-RILP, HA-RILP $\Delta$ C2, HA-RILPC33, Myc-Rab7, and V1G1 in different combinations and we immunoprecipitated V1G1 using a specific anti-V1G1 antibody (Fig. 6D). Immunoprecipitates were then analyzed for the presence of the different recombinant proteins. As expected V1G1 was able to co-immunoprecipitate HA-RILP, HA-RILP $\Delta$ C2 but not HA-RILPC33 (Fig. 6D, lanes 2-4). Interestingly, V1G1 was also able to co-immunoprecipitate Rab7 (Fig. 6D, lane 5) although in the two-hybrid system we did not detect interaction between these two proteins (Fig. S1). However, coimmunoprecipitation of V1G1 and Rab7 was seen both upon exogenous HA-RILP expression (Fig. 6D, lane 7) and in the presence of endogenous RILP (Fig. 6D, lane 5). In RILP-silenced cells Rab7 was not anymore co-immunoprecipitating with V1G1 (Fig. 6D, lane 6). These data indicate that V1G1 does not interact directly with Rab7 and that RILP is able to interact simultaneously with Rab7 and V1G1. Indeed, expression of RILP truncated forms RILP $\Delta$ C2 or RILPC33, binding to and sequestering V1G1 and Rab7 respectively, abolished the co-immunoprecipitation of Rab7 (Fig. 6D, 12-13).

Altogether these data indicate that Rab7 recruits on endolysosomal membranes RILP that in turn recruit V1G1, while RILP induces V1G1 proteasomal degradation when it is not bound to Rab7.

### **V-ATPase activity is regulated by RILP**

RILP is required for biogenesis of multivesicular bodies (MVBs) and, together with Rab7, regulates late endocytic traffic (Progida et al., 2007). Acidification, triggered by V-ATPase, is required for the formation of MVBs (Aniento et al., 1996; Clague et al., 1994; Marshansky and Futai, 2008; Trajkovic et al., 2008). Thus RILP might coordinate the biogenesis of MVBs through V-ATPase activity regulation, by controlling V1G1 amount and localization. In order to investigate if RILP influence V-ATPase activity we used LysoTracker Red, a marker of acidic compartments that stains vesicles with an internal pH of less than 6.5, in HeLa cells depleted of RILP (RILPi) (Fig. 7A). The samples were analyzed by live microscopy and LysoTracker Red intensity in RILPi samples relative to control (scr) was quantified (Fig. 7B). Interestingly, the levels of LysoTracker Red intensity increased more than twice in RILPi cells, suggesting a role of RILP in controlling V-ATPase activity (Fig. 7A, B).

Furthermore, the distribution of acidic compartments was more diffuse and peripheral in RILP-depleted cells compared to control cells (scr).

### **V1G1 is fundamental for V-ATPase activity**

Since we have demonstrated that RILP is important for acidification and controls V1G1 abundance and recruitment on late endosomal and lysosomal membranes, we decided to investigate the relevance of V1G1 on V-ATPase activity. In order to monitor how variations of V1G1 abundance affect V-ATPase activity, we monitored cathepsin D maturation in HeLa cells overexpressing V1G1 or silenced for V1G1 both transiently and stably. Cathepsin D is synthesized as preprocathepsin-D precursor, which is converted into procathepsin D (52 kDa) in the endoplasmic reticulum (ER) and then it undergoes further proteolytic processing, in the acidic milieu of late endosomes and lysosomes, being converted in a 44-kDa form and finally into the 32-kDa mature form. Lysates of control HeLa cells, of V1G1-silenced or of V1G1 overexpressing cells were subjected to Western blot analysis with an anti-cathepsin D antibody able to recognize the 52 kDa, the 44 kDa and the 32 kDa forms (Fig. 7C). In control cells the 52 kDa and the 44 kDa represented less than 30% of the total cathepsin D staining while, as expected, treatment with the high affinity inhibitor of V-ATPase bafilomycin A1 caused the accumulation of the immature forms and reduced the amount of the mature 32 kDa form to less than 5% (Fig. 7C, D). Transient or stable overexpression (in two independent clones) of V1G1 caused a strong increase in the amount of immature cathepsin D forms while the mature 32 kDa form represented less than 25% of the total cathepsin D staining (Fig. 7C, D). Similarly, transient or stable depletion of V1G1 (in two independent clones) caused an accumulation of the immature forms while the mature cathepsin D 32 kDa form was less than 25% of the total cathepsin D staining (Fig. 7C, D). In contrast, no changes were detected in cells transfected with a construct expressing a control sh-RNA (Fig. 7C, D).

As V1G1 seems to be important to ensure a proper V-ATPase activity, we wanted to investigate the effect on late endosomes and lysosomes when cells were depleted of V1G1. We therefore used two different markers of acidic compartments: LysoTracker Red (that accumulates in acidic compartments) and LysoSensor DND-192 (that labels less acidic compartments than LysoTracker Red) and we internalized fluorescently labeled transferrin in HeLa cells stable depleted of V1G1 (in two

independent clones). Afterwards, we quantified the relative amount of transferrin colocalizing with LysoTracker Red or LysoSensor-positive endosomes, by confocal microscopy analysis (Fig. S2). Transferrin labels mainly sorting and recycling early endosomes and only a little percentage of it reach late endosomes and lysosomes to be degraded (Dautry-Varsat et al., 1983; Hopkins and Trowbridge, 1983). Changes in the percentage of transferrin colocalizing with endocytic degradative compartments represent a clear indication of alteration of the endocytic route (Roxrud et al., 2009). The levels of transferrin in LysoTracker-positive structures increased in both clones depleted of V1G1, and the increase was stronger in LysoSensor-positive endosomes (Fig. S2). These results confirm the importance of V1G1 for the V-ATPase activity, as the depletion of this subunit causes accumulation of transferrin in acidic compartments, suggesting impaired degradation, and thus malfunctioning of late endosomes and lysosomes.

Altogether, these data demonstrate that changes in the amount of V1G1 impair V-ATPase activity.

## Discussion

V-ATPases are highly conserved enzymes that couple ATP hydrolysis to proton transport across membranes, are constituted by two domains and multiple subunits and are localized to the membrane of several organelles (Cipriano et al., 2008; Toei et al., 2010). The G subunit of the V-ATPase V1 domain is part, together with the E subunit, of the peripheral stator stalks responsible for structurally and functionally linking the peripheral V1 sector to the membrane VO sector of the pump (Armbrüster et al., 2003; Ohira et al., 2006). There are two isoforms of the G subunit: G1 is ubiquitously distributed while G2 is specifically localized in central nervous system neurons (Murata et al., 2002). We have identified the G1 subunit of V-ATPase as a RILP interacting protein. We proved that the interaction is physiological as it was detected by co-immunoprecipitation of overexpressed (Fig. 1A) but also endogenous proteins (Fig. 1C). Furthermore, we proved that the interaction is direct, as it was detectable also between bacterially expressed and purified proteins (Fig. 1D). In addition, our data indicate that V1G1 interacts with the N-terminal half of RILP (Fig. 1, 6D, S1,) in contrast to Rab7 that binds in the C-terminal half of RILP (Cantalupo et al., 2001). Interestingly, the complex RILP-V1G1 can interact with the dynactin

projecting arm p150<sup>Glued</sup> (Fig. 1E), suggesting that RILP could control simultaneously endosomes acidification and translocation toward the microtubule organizing center.

Which is the functional meaning of this interaction?

Our data indicate that RILP regulates recruitment of V1G1 on endosomes and lysosomes. Overexpression of RILP increases colocalization of V1G1 with the late endosomal/lysosomal marker Lamp1 while expression of the RILPC33 mutant, unable to bind V1G1, decreases it (Fig. 4). In addition, overexpression of RILP increases the amount of V1G1 present in membranes and drastically decreases V1G1 in the cytosol (Fig. 3A, B). In agreement, in RILP-silenced cells colocalization of V1G1 with Lamp1 decreases while co-localization with giantin increases (Fig. 5) indicating that RILP is important for recruitment of V1G1 on late endosomal and lysosomal membranes. Thus, GTP-bound Rab7 recruits RILP on late endosomes and lysosomes (Cantalupo et al., 2001) and RILP, in turn, recruits V1G1 on these organelles. In fact, we demonstrated by co-immunoprecipitation that RILP is able to bind simultaneously V1G1 at its N-terminal half and Rab7 at its C-terminal half (Fig. 6D). Also we established that V1G1 is not able to bind directly Rab7 since V1G1 is not able to interact with Rab7 in the two-hybrid system (Fig. S1) and it is not able to co-immunoprecipitate Rab7 in the absence of RILP (Fig. 6D).

As V1G1 is important for V-ATPase assembly and function (Ohira et al., 2006; Tomashek et al., 1997), the recruitment of V1G1 on endosomal/lysosomal membranes is likely to contribute to the correct assembly and, consequently, functioning of the pump. In fact our data show that V1G1, when binding to RILP, can be also in complex with other subunits of the cytosolic and membrane domain of V-ATPase (Fig. 3C), thus suggesting that RILP could control not only recruitment of V1G1 on endosomal and lysosomal membranes but also the assembly of the entire pump. Furthermore, we demonstrated that RILP modulates the activity of the pump on late endosomes and lysosomes controlling V1G1 localization (Fig. 4, 5). Indeed, in RILP-depleted cells we detected mislocalization of the V1G1 on other organelles (Fig. 5) and a different intracellular distribution and higher intensity of LysoTracker Red (Fig. 7A-B). These data, together with the previously reported inhibition of EGFR degradation and increase of Lamp levels upon RILP silencing (Progida et al., 2006; Progida et al., 2007), suggest a block of endosomal maturation caused by the failed recruitment of the proton pump on Rab7-labeled endosomes.

We have shown previously that RILP is important for MVBs formation (Progida et al., 2007; Progida et al., 2006). As MVBs formation is dependent on the luminal acidic pH of endosomes and thus on the acidification triggered by V-ATPase (Aniento et al., 1996; Clague et al., 1994; Marshansky and Futai, 2008; Trajkovic et al., 2008), our data support the idea that RILP might coordinate the biogenesis of MVBs through V1G1 activity regulation.

Our data demonstrate also that RILP regulates V1G1 subunit abundance. Overexpression of RILP causes a reduction of V1G1 amount while in RILP-silenced cells the V1G1 amount is strongly increased (Fig. 2A, B). Furthermore, we established that RILP induces V1G1 ubiquitination-dependent proteasomal degradation (Fig. 2I). Thus, RILP promotes recruitment of V1G1 on endosomal membranes but also induces V1G1 degradation. How are these two different and contrasting functions regulated? Our data indicate that overexpression of Rab7 has no effect on V1G1 abundance while Rab7 silencing causes a strong V1G1 decrease (Fig. 6A, B). Hence these data suggest that when RILP is bound to Rab7 recruits V1G1 on membranes, while an excess of RILP unbound to Rab7 (as in the case of RILP overexpression or of Rab7 silencing) leads to V1G1 degradation. Therefore, the amount of V1G1 is strictly regulated by the availability of cytosolic RILP.

Previously, we have observed that expression of the Rab7T22N mutant, which is unable to recruit RILP on late endosomal/lysosomal membranes, causes a strong decrease in LysoTracker Red staining (Bucci et al., 2000), thus indicating an increase in pH of intracellular organelles, possibly caused by impaired V-ATPase assembly and function due to the lack of recruitment of V1G1 mediated by RILP. These data seem in contrast with the fact that RILP silencing causes an increase of LysoTracker intensity (Fig. 7A, B). However, in cells expressing the Rab7T22N mutant, RILP is still present but it can't be recruited on endosomes and could, instead, induce V1G1 degradation.

We also demonstrated that a proper amount of V1G1 seems to be fundamental for the correct functioning of the pump. Overexpression or silencing of V1G1 subunit causes a strong inhibition of cathepsin D maturation similarly to what happens treating the cells with BafilomycinA1, a inhibitor of the vacuolar pump (Fig. 7C, D). Moreover, V1G1 silencing causes accumulation of transferrin in acidic compartments suggesting malfunctioning of late endosomes and lysosomes (Fig. S2). These data are in agreement with previously published data suggesting that changes in V1G1

expression destabilizes the E subunit influencing V-ATPase assembly (Ohira et al., 2006; Tomashek et al., 1997). The V1G1 subunit thus seems to be a crucial subunit not only for correct assembly of the vacuolar pump but also for V-ATPase function as changes in V1G1 amounts have strong negative effects on processes regulated by V-ATPase.

The discovery of the interaction between RILP and V1G1 is of importance as it reveals a new mechanism of regulation of the V-ATPase mediated by RILP. In particular, our data demonstrate that RILP regulates V1G1 abundance and it is crucial for the regulation of V-ATPase at the level of late endosomes and lysosomes promoting assembly and activation of the proton pump on these organelles (Fig. 8).

V-ATPase has been proposed as a drug target for several diseases and processes (Hinton et al., 2009; Kartner and Manolson, 2012). Plasma membrane V-ATPases are important for sperm maturation and viability (Pietrement et al., 2006), for acid secretion of certain kind of renal cells whose malfunctioning causes renal tubular acidosis (Karet et al., 1999; Smith et al., 2000), and for osteoclast bone degradation (Frattini et al., 2000; Toyomura et al., 2003) that, if altered, causes osteopetrosis and osteoporosis. Importantly, in many tumor cell lines V-ATPases are abundant in plasma membranes and activity in plasma membranes has been directly correlated with invasiveness (Sennoune et al., 2004a; Sennoune et al., 2004b; Sennoune and Martinez-Zaguilan, 2012). The tumor acidic microenvironment has a key role for tumor development and progression as it influences resistance to chemotherapy, proliferation and formation of metastasis (Hernandez et al., 2012). Thus, in order to fight cancer, the use of V-ATPase inhibitors and/or the regulation of V-ATPase assembly have been proposed to control V-ATPase activity (Kane, 2012; Pérez-Sayáns et al., 2009). Our data suggest that modulation of RILP expression could represent a mechanism to regulate V-ATPase activity. Furthermore, the discovery of the functional link between RILP and V-ATPase opens new scenarios on the cellular role of RILP that will have to be further investigated.

## **Materials and methods**

### **Cells and reagents**

Restriction and modification enzymes were from New England Biolabs (Ipswich, MA), chemicals were from Sigma-Aldrich (St Luis, MO), while tissue culture

reagents were from Sigma-Aldrich or Invitrogen (Carlsbad, CA). HeLa cells were grown in DMEM supplemented with 10% FBS, 2 mM glutamine, 100 U/ml penicillin and 10 mg/ml streptomycin, in a 5% CO<sub>2</sub> incubator at 37°C. HeLa cells were also stably transfected with pCDNA3\_2xHA\_V1G1 plasmid or stably silenced using the sh-RNA V1G1 plasmids (sc-36797-SH, Santa Cruz Biotechnology, Santa Cruz, CA). Stable cell lines were selected adding G-418 (1mg/ml, Calbiochem, Darmstadt, Germany) to cells transfected with pCDNA3\_2xHA\_V1G1 plasmid or Puromycin (3µg/ml, Sigma-Aldrich) to V1G1- silenced cells. When indicated MG132 (10µM, C2211 Sigma-Aldrich) was used for 3-5h.

### Plasmid construction

Most Rab7 and RILP constructs used in this study have been described previously (Cantalupo et al., 2001; Colucci et al., 2005a; Progida et al., 2006; Vitelli et al., 1997). The pCDNA3\_2xHA\_RILP construct was used to amplify a fragment using the following oligonucleotides 5'-CTTAGAATTCTAATGGAGCCCAGGAGGGCGGCG-3' and 5'-ATAAGAATGCGGCCGCTCACCATTTCGGGCTCCTGTCCGTGCTG-3'. The fragment, coding for the N-terminal half of RILP, was then digested with EcoRI and NotI and cloned in the pCDNA3-2xHA vector to obtain a construct for the expression of a HA-tagged RILPΔC2. The V1G1 ORF was amplified from the two-hybrid pACT2-V1G1 construct using the following oligonucleotides 5'-CTAAGATCTATGGCTAGTCAGTCTCAGGGG-3' and 5'-CGCAAGCTTCTATCCATTTATGCGGTAGTT-3'. The amplified fragment was then digested with BglII and HindIII and cloned in the pEGFP-C1 vector to obtain a construct for expression of GFP-tagged V1G1. The pCDNA3-V1G1 construct was obtained after cloning the BglII-HindIII fragment from the pEGFP-V1G1 in the pCDNA3 vector cut with BamHI and HindIII. To obtain the HA-tagged V1G1 an EcoRV-XhoI fragment containing the V1G1 ORF was cloned in the pCDNA3\_2xHA plasmid. The pCMV6-AC-GFP-V1G1 (RG203317) were obtained from Origene (Rockville, MD). The pEF-FLAG-p150<sup>Glued</sup> construct has been previously described (Ohbayashi et al., 2012).

### Two-hybrid assay

The construct pGBKT7-RILP was used to screen a human liver cDNA library in the



pACT2 vector in AH109 yeast cells (Bartel et al., 1993; Suter et al., 2008). Transformants were plated onto synthetic medium lacking His, Leu, and Trp. Colonies were picked 5 days later and then assayed for growth on medium lacking Ade, His, Leu and Trp and for  $\beta$ -galactosidase activity (Bartel et al., 1993). Specificity tests were made transforming AH109 yeast cells with the pGBKT7 vector or the pGBKT7-Rab7 construct (as a negative controls) or the pGBKT7-RILP wt construct, and with the PGADT7-V1G1 construct. Clones were then assayed for growth on selective medium and for  $\beta$ -galactosidase activity using o-nitrophenyl- $\beta$ -D-galactoside as a substrate (Bartel et al., 1993).

### Transfection and RNA interference

Transfection was performed using Metafectene Pro or Metafectene Easy from Biontex (Martinsried, Germany) following manufacturer's instructions. After 20 h of transfection cells were processed for immunofluorescence or biochemical assays. For RNA interference siRNAs were purchased from MWG-Biotech (Ebersberg, Germany) or Sigma-Aldrich. We used the following oligonucleotides: siRNA-RILP2, sense 5'-GAUCAAGGCCAAGAUGUUATT-3' and antisense sequence 5'-UAACAUCUUGGCCUUGAUCTT-3'; control RNA: sense 5'-ACUUCGAGCGUGCAUGGCUTT-3' and antisense 5'-AGCCAUGCACGCUCGAAGUTT-3'; siRNA-V1G1, sense 5'-AGAAGAAGCUCAGGCUGAATT-3' and antisense sequence 5'-UUCTGCCTGAGCUUCUUCUTT-3'; siRNA-Rab7a, sense 5'-GGAUGACCUCUAGGAAGAATT-3' and antisense sequence 5'-UUCUUCCUAGAGGUCAUCCTT-3'. RILP and Rab7 siRNA were efficient in silencing as previously reported (De Luca et al., 2008; Progida et al., 2007; Spinosa et al., 2008). Briefly, HeLa cells were plated 1 day before transfection in tissue culture dishes (6 cm diameter). Cells were transfected with siRNAs using Oligofectamine from Invitrogen for 72 h, re-plated and left 48 h before performing further experiments.

### Antibodies

Rabbit anti-RILP polyclonal antibodies have been previously described (Cantalupo et al., 2001). Goat polyclonal anti-RILP (1:100, sc-82746), rabbit



polyclonal anti-RILP (1:100, sc-98331), mouse monoclonal 9E10 anti-Myc (1:500, sc-40), rabbit polyclonal and mouse monoclonal anti-HA (1:500, sc-805 and sc-7392 respectively), mouse monoclonal anti-V1G1 (1:100, sc-25333), mouse monoclonal anti-V0D1 (1:100, sc-81887), goat polyclonal anti-Cathepsin D (1:500, sc-6486) and rabbit polyclonal anti-GAPDH (1:10000, sc-25778) antibodies were from Santa Cruz Biotechnology. Rabbit polyclonal anti-V1C1 (1:1000, 361-375), rabbit polyclonal anti-Rab7 (1:1000, R4779), mouse monoclonal anti-Rab7 (1:1000, R8779) and mouse monoclonal anti-tubulin (1:3000, clone B512) were from Sigma-Aldrich. Chicken polyclonal anti-V1G1 (1:1000, ab15853) and rabbit polyclonal anti-Giantin (1:1000, ab24586) were from Abcam (Cambridge, UK). Goat polyclonal anti-GST (1:2000, 27-4577-01) was from GE Healthcare (Buckinghamshire, UK) and rabbit polyclonal anti-ubiquitin (1:5000, Z0458) was from DAKO (Glostrup Denmark). Mouse monoclonal anti-p150 (1:500, 610474) was from BD Bioscience. Secondary antibodies conjugated with fluorochromes or HRP were from Invitrogen or SantaCruz Biotechnology.

### **Membrane-cytosol separation**

For cytosolic and membrane distribution, pellets of HeLa cells were dissolved with homogenization buffer (8% sucrose in 3mM imidazole). Cells were passed through a 26 gauge needle and centrifuged at 3800g for 5 min at 4°C. The supernatant (PNS) was centrifuged at 20000rpm for 2h at 4°C and fractionated into high-speed pellet (membrane) and supernatant (cytosol).

### **Co-immunoprecipitation, pull-down and direct interaction experiments**

For immunoprecipitation we used anti-HA affinity gel (Ezview Red Anti-HA E6779 from Sigma) accordingly to manufacturer indications and as previously described (Cogli et al., 2013b). Co-immunoprecipitation of endogenous proteins in HeLa cells was performed using a crosslink immunoprecipitation kit (Pierce, Rockford, USA) following manufacturer instructions and as previously described (Cogli et al., 2013a).

For direct interaction GST, GST-tagged and His-tagged proteins were expressed in bacteria and affinity purified as described (Chiariello et al., 1999). Glutathione resin alone or bound to purified GST, GST-RILPC33 or GST-RILP was incubated with purified His-tagged V1G1 in PBS with 2 mM MgCl<sub>2</sub> and GTP 0.8 mM for 1 h on a rotating wheel. Subsequently, samples were subject to GST pull-

down using the glutathione resin. Samples were then subjected to SDS-PAGE and Western blotting. Pull-down experiments were previously described (Cogli et al., 2013b). Briefly, purified His-V1G1 was bound to Ni-NTA resin and incubated with lysates of HeLa cells transfected with FLAG-p150<sup>Glued</sup> in the presence or absence of purified GST-RILP for 2h at 4°C. In addition, as a control, purified GST-RILP was bound to Glutathione resin and incubated with lysates of HeLa cells transfected with FLAG-p150<sup>Glued</sup> for 2h at 4°C. After incubation samples were processed for SDS-PAGE and Western blot analysis.

### **Western blotting**

HeLa cells were lysed with RIPA buffer (R0278, Sigma-Aldrich) plus proteinase inhibitors cocktail (Roche, Mannheim Germany). For ubiquitination experiments RIPA buffer was supplemented with 20 mM Na pyrophosphate pH 7.5, protease inhibitors cocktail (Roche), 50 mM NaF, 2 mM PMSF, 10 mM Na vanadate in HEPES pH 7.5 and 5 µM NEM (N-ethylmaleimide). Lysates were loaded on SDS-PAGE and separated proteins were transferred onto PVDF membrane from Millipore (Billerica, MA, USA).

The filter was blocked in 5% milk in PBS for 30 minutes at room temperature, incubated with the appropriate antibody and then with a secondary antibody conjugated with HRP (diluted 1:5000).

For anti-ubiquitin incubation, after transferring, filter was subjected to a treatment in denaturing solution (6M guanidium chloride, 20 mM Tris pH 7.4, 1 mM PMSF, β-mercaptoethanol) for 30 minutes at 4°C, to make proteins more accessible to the antibody. After extensive washing in TBS-T buffer (25mM Tris, 150 mM NaCl pH 8, Tween 0,05%) the filter was blocked in 5% BSA in TBS (25mM Tris, 150 mM NaCl pH 8) for 30 min at room temperature, incubated with the anti-ubiquitin antibody and then with a secondary antibody conjugated with HRP (diluted 1:5000).

Bands were visualized using Western blot Luminol Reagent (Santa Cruz) or SuperSignal West Pico (Pierce).

### **Confocal immunofluorescence microscopy**

Cells grown on 11-mm round glass coverslips were permeabilized, fixed and incubated with the antibodies as described previously (Bucci et al., 1992). Cells were

viewed with Zeiss LSM 510 confocal microscope. In some experiments cells were incubated with LysoTrackerRed or LysoSensor DND-192 (Invitrogen) and Alexa647- or Alexa555-labelled transferrin (Invitrogen) for 30 min. Cells were imaged by live microscopy, and the relative level of transferrin colocalizing with LysoTracker or LysoSensor was quantified.

### Standard RNA procedures and quantitative real-time PCR

Total RNA was extracted from HeLa cells using RNeasy mini kit according to the manufacturer's instructions (Qiagen, Hilden, Germany). The RNA retrotranscription protocol was performed as described (Progida et al., 2010). Quantitative real-time PCR was performed using SYBR Green JumpStart ReadyMix (Sigma) in the Smart Cycler II Real-Time PCR detection system (Cepheid, Sunnyvale, CA, USA). The primers used GAPDH *Forward*: 5'-GGTGGTCTCCTCTGACTTCAACA-3' *Reverse*: 5'-GTTGCTGTAGCCAAATTCGTTGT-3'; V<sub>1</sub>G<sub>1</sub> *Forward*: 5'-GCCGAGAAGGTGTCCGAGGCCCG-3' *Reverse*: 5'-GCGGTACTGTTCAATTCAGCC-3'; RILP *Forward*: 5'-CGGAAGCAGCGGAAGAAGATCAAG-3' *Reverse*: 5'-GAGCAGGATCCATGGGCCAGC-3' were purchased from Eurofin MWG Operon (Ebersberg, Germany). The PCR programme was as follows: 1 cycle 3 minutes at 94°C; 35 cycles 30 seconds at 94°C, 30 seconds at 60°C, 30 seconds at 72°C; 1 cycle 6 minutes at 75°C. The specificity of PCR products was checked by performing a melting-curve test.

### Acknowledgements

We thank Anna Maria Rosaria Colucci for help in the first two-hybrid screening and Mitsunori Fukuda for kindly donating pEF-FLAG-p150<sup>Glued</sup> plasmid. The financial support of AIRC (Associazione Italiana per la Ricerca sul Cancro, Investigator Grant N. 10213 and 14709 to C. B.), Telethon-Italy (Grant N. GGP09045 to C.B.) and of MIUR (PRIN2010-2011 and ex60% to C.B.) is gratefully acknowledged. M.D.L. is a recipient of a triennial FIRC (Fondazione Italiana per la ricerca sul cancro) fellowship. *Author contributions*: MDL, LC, CP and VN performed experiments. RP, SS and PPDF provided reagents, expertise and support for the ubiquitination experiment. MDL

and CB conceived or designed the experiments and analyzed the results. CB wrote the manuscript.

The authors declare that they have no conflicting financial interest.

## References

- Aloisi, A.L., Bucci, C.** (2013). Rab GTPases-cargo direct interactions: fine modulators of intracellular trafficking. *Histol Histopathol.* **28**, 839-849.
- Aniento, F., Gu, F., Parton, R.G., Gruenberg, J.** (1996). An endosomal •-COP is involved in the pH-dependent formation of transport vesicles destined for late endosomes. *J Cell Biol.* **133**, 29-41.
- Armbrüster, A., Bailer, S.M., Koch, M.H., Godovac-Zimmermann, J., Grüber, G.** (2003). Dimer formation of subunit G of the yeast V-ATPase. *FEBS Lett.* **546**, 395-400.
- Bartel, P., Chien, C.T., Sternglanz, R., Fields, S.** (1993). Elimination of false positives that arise in using the two-hybrid system. *Biotechniques.* **14**, 920-924.
- Bucci, C., Chiariello, M.** (2006). Signal transduction gRABs attention. *Cell Signal.* **18**, 1-8.
- Bucci, C., Frunzio, R., Chiariotti, L., Brown, A.L., Rechler, M.M., Bruni, C.B.** (1988). A new member of the ras gene superfamily identified in a rat liver cell line. *Nucleic Acids Res.* **16**, 9979-93.
- Bucci, C., Parton, R.G., Mather, I.H., Stunnenberg, H., Simons, K., Hoflack, B., Zerial, M.** (1992). The small GTPase rab5 functions as a regulatory factor in the early endocytic pathway. *Cell.* **70**, 715-728.
- Bucci, C., Thomsen, P., Nicoziani, P., McCarthy, J., van Deurs, B.** (2000). Rab7: a key to lysosome biogenesis. *Mol Biol Cell.* **11**, 467-480.
- Cantalupo, G., Alifano, P., Roberti, V., Bruni, C.B., Bucci, C.** (2001). Rab-interacting lysosomal protein (RILP): the Rab7 effector required for transport to lysosomes. *EMBO J.* **20**, 683-693.
- Casey, J., Grinstein, S., Orlowski, J.** (2010). Sensors and regulators of intracellular pH. *Nat Rev Mol Cell Biol.* **11**, 50-61.
- Chavrier, P., Parton, R.G., Hauri, H.P., Simons, K., Zerial, M.** (1990). Localization of low molecular weight GTP binding proteins to exocytic and endocytic compartments. *Cell.* **62**, 317-29.
- Chiariello, M., Bruni, C.B., Bucci, C.** (1999). The small GTPases Rab5a, Rab5b and Rab5c are differentially phosphorylated in vitro. *FEBS Lett.* **453**, 20-24.
- Cipriano, D.J., Wang, Y., Bond, S., Hinton, A., Jefferies, K.C., Qi, J., Forgac, M.** (2008). Structure and regulation of the vacuolar ATPases. *Biochim Biophys Acta.* **1777**, 599-604.

**Clague, M.J., Urbe, S., Aniento, F., Gruenberg, J.** (1994). Vacuolar ATPase activity is required for endosomal carrier vesicle formation. *J Biol Chem.* **269**, 21-24.

**Cogli, L., Progida, C., Bramato, R., Bucci, C.** (2013a). Vimentin phosphorylation and assembly are regulated by the small GTPase Rab7a. *Biochim Biophys Acta.* **1833**, 1283-1293.

**Cogli, L., Progida, C., Thomas, C.L., Spencer-Dene, B., Donno, C., Schiavo, G., Bucci, C.** (2013b). Charcot-Marie-Tooth type 2B disease-causing RAB7A mutant proteins show altered interaction with the neuronal intermediate filament peripherin. *Acta Neuropathol.* **125**, 257-272.

**Colucci, A.M.R., Campana, M.C., Bellopede, M., Bucci, C.** (2005a). The Rab-interacting lysosomal protein, a Rab7 and Rab34 effector, is capable of self-interaction. *Biochem Biophys Res Commun.* **334**, 128-133.

**Colucci, A.M.R., Spinosa, M.R., Bucci, C.** (2005b). Expression, assay and functional properties of RILP. *Methods Enzymol.* **403**, 664-675.

**Dautry-Varsat, A., Ciechanover, A., Lodish, H.F.** (1983). pH and the recycling of transferrin during receptor-mediated endocytosis. *Proc Natl Acad Sci USA.* **80**, 2258-2262.

**De Luca, A., Progida, C., Spinosa, M.R., Alifano, P., Bucci, C.** (2008). Characterization of the Rab7K157N mutant protein associated with Charcot-Marie-Tooth type 2B. *Biochem Biophys Res Commun.* **372**, 283-287.

**Diakov, T.T., Kane, P.M.** (2010). Regulation of V-ATPase activity and assembly by extracellular pH. *J Biol Chem.* **285**, 23771-23778.

**El Far, O., Seagar, M.** (2011). A role for V-ATPase subunits in synaptic vesicle fusion? *J Neurochem.* **117**, 603-612.

**Forgac, M.** (2007). Vacuolar ATPases: rotary proton pumps in physiology and pathophysiology. *Nat Rev Mol Cell Biol.* **8**, 917-929.

**Frattoni, A., Orchard, P.J., Sobacchi, C., Giliani, S., Abinun, M., Mattsson, J.P., Keeling, D.J., Andersson, A.K., Wallbrandt, P., Zecca, L. et al.** (2000). Defects in TCIRG1 subunit of the vacuolar proton pump are responsible for a subset of human autosomal recessive osteopetrosis. *Nat Genet.* **25**, 343-346.

**Hernandez, A., Serrano-Bueno, G., Perez-Castineira, J.R., Serrano, A.** (2012). Intracellular proton pumps as targets in chemotherapy: V-ATPases and cancer. *Curr Pharm Des.* **18**, 1383-1394.

**Harrison, R.E., Bucci, C., Vieira, O.V., Schroer, T.A., Grinstein, S.** (2003). Phagosomes fuse with late endosomes and/or lysosomes by extension of membrane protrusions along microtubules: role of Rab7 and RILP. *Mol Cell Biol.* **23**, 6494-506.

**Hinton, A., Bond, S., Forgac, M.** (2009). V-ATPase functions in normal and disease processes. *Pflugers Arch.* **457**, 589-598.

**Hopkins, C.R., Trowbridge, I.S.** (1983). Internalization and processing of transferrin and the transferrin receptor in human carcinoma A431 cells. *J Cell Biol.* **97**, 508-521.

**Hurtado-Lorenzo, A., Skinner, M., El Annan, J., Futai, M., Sun-Wada, G.H., Bourgoin, S., Casanova, J., Wildeman, A., Bechoua, S., Ausiello, D.A. et al.** (2006). V-ATPase interacts with ARNO and Arf6 in early endosomes and regulates the protein degradative pathway. *Nat Cell Biol.* **8**, 124-136.

**Jordens, I., Fernandez-Borja, M., Marsman, M., Dusseljee, S., Janssen, L., Calafat, J., Janssen, H., Wubbolts, R., Neefjes, J.** (2001). The Rab7 effector protein RILP controls lysosomal transport by inducing the recruitment of dynein-dynactin motors. *Curr Biol.* **11**, 1680-1685.

**Johansson, M., Rocha, N., Zwart, W., Jordens, I., Janssen, L., Kuijl, C., Olkkonen, V.M., Neefjes, J.** (2007). Activation of endosomal dynein motors by stepwise assembly of Rab7-RILP-p150<sup>Glued</sup>, ORP1L, and the receptor betalll spectrin. *J Cell Biol.* **176**, 459-71.

**Kane, P.M.** (2006). The where, when, and how of organelle acidification by the yeast vacuolar H<sup>+</sup>-ATPase. *Microbiol Mol Biol Rev.* **70**, 177-191.

**Kane, P.M.** (2012). Targeting reversible disassembly as a mechanism of controlling V-ATPase activity. *Curr Protein Pept Sci.* **13**, 117-123.

**Kane, P.M., Smardon, A.M.** (2003). Assembly and regulation of the yeast vacuolar H<sup>+</sup>-ATPase. *J Bioenerg Biomembr.* **35**, 313-321.

**Karet, F.E., Finberg, K.E., Nelson, R.D., Nayir, A., Mocan, H., Sanjad, S.A., Rodriguez-Soriano, J., Santos, F., Cremers, C.W., Di Pietro, A. et al.** (1999). Mutations in the gene encoding B1 subunit of H<sup>+</sup>-ATPase cause renal tubular acidosis with sensorineural deafness. *Nat Genet.* **21**, 84-90.

**Kartner, N., Manolson, M.F.** (2012). V-ATPase subunit interactions: the long road to therapeutic targeting. *Curr Protein Pept Sci.* **13**, 164-179.

**Marshansky, V., Futai, M.** (2008). The V-type H<sup>+</sup>-ATPase in vesicular trafficking: targeting, regulation and function. *Curr Opin Cell Biol.* **20**, 415-426.

**Murata, Y., Sun-Wada, G.H., Yoshimizu, T., Yamamoto, A., Wada, Y., Futai, M.** (2002). Differential localization of the vacuolar H<sup>+</sup> pump with G subunit isoforms (G1 and G2) in mouse neurons. *J Biol Chem.* **277**, 39296-39303.

**Ohbayashi, N., Yatsu, A., Tamura, K., Fukuda, M.** (2012) The Rab21-GEF activity of Varp, but not its Rab32/38 effector function, is required for dendrite formation in melanocytes. *Mol Biol Cell.* **23**, 669-78.

- Ohira, M., Smardon, A.M., Charsky, C.M., Liu, J., Tarsio, M., Kane, P.M.** (2006). The E and G subunits of the yeast V-ATPase interact tightly and are both present at more than one copy per V1 complex. *J Biol Chem.* **281**, 22752-22760.
- Pérez-Sayáns, M., Somoza-Martín, J.M., Barros-Angueira, F., Rey, J.M., García-García, A.** (2009). V-ATPase inhibitors and implication in cancer treatment. *Cancer Treat Rev.* **35**, 707-713.
- Pietrement, C., Sun-Wada, G.H., Silva, N.D., McKee, M., Marshansky, V., Brown, D., Futai, M., Breton, S.** (2006). Distinct expression patterns of different subunit isoforms of the V-ATPase in the rat epididymis. *Biol Reprod.* **74**, 185-194.
- Progida, C., Spinosa, M., De Luca, A., Bucci, C.** (2006). RILP interacts with the VPS22 component of the ESCRT-II complex. *Biochem Biophys Res Commun.* **347**, 1074-1079.
- Progida, C., Malerød, L., Stuffers, S., Brech, A., Bucci, C., Stenmark, H.** (2007). RILP is required for proper morphology and function of late endosomes. *J Cell Sci.* **120**, 3729-3737.
- Progida, C., Cogli, L., Piro, F., De Luca, A., Bakke, O., Bucci, C.** (2010). Rab7b controls trafficking from endosomes to the TGN. *J Cell Sci.* **123**, 1480-1491.
- Qi, J., Wang, Y., Forgac, M.** (2007). The vacuolar (H<sup>+</sup>)-ATPase: subunit arrangement and in vivo regulation. *J Bioenerg Biomembr.* **39**, 423-426.
- Qiu, Q.S.** (2012). V-ATPase, ScNhx1p and yeast vacuole fusion. *J Genet Genomics.* **39**, 167-171.
- Roxrud, I., Raiborg, C., Gilfillan, G.D., Strømme, P., Stenmark, H.** (2009). Dual degradation mechanisms ensure disposal of NHE6 mutant protein associated with neurological disease. *Exp Cell Res.* **315**, 3014-3027.
- Sennoune, S.R., Bakunts, K., Martínez, G.M., Chua-Tuan, J.L., Kebir, Y., Attaya, M.N., Martínez-Zaguilán, R.** (2004a). Vacuolar H<sup>+</sup>-ATPase in human breast cancer cells with distinct metastatic potential: distribution and functional activity. *Am J Physiol Cell Physiol.* **286**, C1443-1452.
- Sennoune, S.R., Luo, D., Martínez-Zaguilán, R.** (2004b). Plasmalemmal vacuolar-type H<sup>+</sup>-ATPase in cancer biology. *Cell Biochem Biophys.* **40**, 185-206.
- Sennoune, S.R., Martinez-Zaguilan, R.** (2012). Vacuolar H<sup>(+)</sup>-ATPase signaling pathway in cancer. *Curr Protein Pept Sci.* **13**, 152-163.
- Smardon, A.M., Tarsio, M., Kane, P.M.** (2002). The RAVE complex is essential for stable assembly of the yeast V-ATPase. *J Biol Chem.* **277**, 13831-13839.
- Smith, A.N., Skaug, J., Choate, K.A., Nayir, A., Bakkaloglu, A., Ozen, S., Hulton, S.A., Sanjad, S.A., Al-Sabban, E.A., Lifton, R.P. et al.** (2000) Mutations in



ATP6N1B, encoding a new kidney vacuolar proton pump 116-kD subunit, cause recessive distal renal tubular acidosis with preserved hearing. *Nat Genet.* **26**, 71-75.

**Spinosa, M.R., Progidia, C., De Luca, A., Colucci, A.M.R., Alifano, P., Bucci, C.** (2008). Functional characterization of Rab7 mutant proteins associated with Charcot-Marie-Tooth type 2B disease. *J Neurosci.* **28**, 1640-1648.

**Stenmark, H.** (2009). Rab GTPases as coordinators of vesicle traffic. *Nat Rev Mol Cell Biol.* **10**, 513-525.

**Sun-Wada, G.H., Wada, Y., Futai, M.** (2004). Diverse and essential roles of mammalian vacuolar-type proton pump ATPase: toward the physiological understanding of inside acidic compartments. *Biochim Biophys Acta.* **1658**, 106-114.

**Suter, B., Kittanakom, S., Stagljär, I.** (2008). Two-hybrid technologies in proteomics research. *Curr Opin Biotechnol.* **19**, 316-323.

**Toeï, M., Saum, R., Forgac, M.** (2010). Regulation and isoform function of the V-ATPases. *Biochemistry.* **49**, 4715-4723.

**Tomashek, J.J., Graham, L.A., Hutchins, M.U., Stevens, T.H., Klionsky, D.J.** (1997). V1-situated stalk subunits of the yeast vacuolar proton-translocating ATPase. *J Biol Chem.* **272**, 26787-26793.

**Toyomura, T., Murata, Y., Yamamoto, A., Oka, T., Sun-Wada, G.H., Wada, Y., Futai, M.** (2003). From lysosomes to the plasma membrane: localization of vacuolar-type H<sup>+</sup>-ATPase with the  $\alpha 3$  isoform during osteoclast differentiation. *J Biol Chem.* **278**, 22023-22030.

**Trajkovic, K., Hsu, C., Chiantia, S., Rajendran, L., Wenzel, D., Wieland, F., Schwille, P., Brugger, B., Simons, M.** (2008). Ceramide triggers budding of exosome vesicles into multivesicular endosomes. *Science.* **319**, 1244-1247.

**Vitelli, R., Santillo, M., Lattero, D., Chiariello, M., Bifulco, M., Bruni, C., Bucci, C.** (1997). Role of the small GTPase Rab7 in the late endocytic pathway. *J Biol Chem.* **272**, 4391-4397.

## Figure legends

**Fig. 1. RILP and V1G1 interact directly.** (A) Lysates of control HeLa cells (NT) or cells expressing HA-RILP, V1G1 or both were subjected to immunoprecipitation using an anti-HA antibody. Lysates (WB) and immunoprecipitates (IP) were subjected to Western blot analysis using anti-HA and anti-V1G1 specific antibodies. (B) Immunoprecipitates obtained using anti-HA antibodies of control HeLa cells (NT) or cells expressing V1G1 and HA-RILP, HA-RILP $\Delta$ C2 or HA-RILPC33 were subjected to Western blot analysis using anti-HA or anti-V1G1 antibody. (C) Total extracts of HeLa cells (WB) and immunoprecipitates (IP) obtained with no antibodies (no ab), with goat anti-RILP or with goat IgG, as indicated, were subjected to WB analysis using chicken anti-V1G1 and rabbit anti-RILP antibodies. (D) Glutathione resin alone or bound to purified GST, GST-RILPC33 or GST-RILP was incubated with purified His-tagged V1G1. After affinity chromatography proteins were subjected to Western blot analysis using anti-GST and anti-V1G1 specific antibodies. (E) Bacterially expressed and purified His-tagged V1G1 was incubated with total extract of HeLa cells expressing FLAG-p150<sup>Glued</sup> in the presence or absence of purified GST-RILP and pulled-down using Ni-NTA resin. As positive control, GST-RILP was pulled down after incubation with total extract of HeLa cells expressing with FLAG-p150<sup>Glued</sup>. Proteins were then loaded on SDS-PAGE and subjected to Western blot analysis using anti-p150<sup>Glued</sup>, anti-V1G1 and anti-GST antibodies.

**Fig. 2. RILP modulates V1G1 abundance in HeLa cells via ubiquitination-dependent proteasomal degradation.** (A) Lysates of control HeLa cells or cells expressing HA-RILP were subjected to Western blot analysis using anti-V1G1, anti-HA, anti-V1C1, anti-V0D1 and anti-tubulin primary antibodies. (B) Cells treated with control RNA (scr), RILP siRNA (RILPi) or V1G1 siRNA (V1G1i) were subjected to Western blot analysis using anti-V1G1, anti-RILP, anti-V1C1, anti-V0D1 and anti-tubulin primary antibodies. (C) Lysates of control HeLa cells (NT) or cells expressing HA-RILP, HA-RILP $\Delta$ C2 or HA-RILPC33 were subjected to Western blot analysis using anti-V1G1, anti-HA and anti-tubulin antibodies. (D) Cells treated with control RNA (scr), RILP siRNA (RILPi) and transfected with HA-RILP as indicated were subjected to Western blot analysis using anti-V1G1, anti-RILP and anti-tubulin

antibodies. **(E-G)** Real Time PCR was performed on control HeLa cells, or cell expressing HA-RILP (RILP1 and RILP2) or silenced for RILP (RILPi1 and RILPi2) and the amount of RILP **(E-F)** or of V1G1 **(G)** was quantified compared to control GAPDH RNA transcript. **(H)** Control cells or cell expressing HA-RILP as indicated were untreated or treated with the proteasomal inhibitor MG132. Lysates were then subjected to Western blot analysis with V1G1, HA and tubulin antibodies. **(I)** Control cells or cells transfected with HA-V1G1 and RILP as indicated were untreated or treated with MG132. Lysates were subjected to Western blot analysis using anti-RILP, anti-V1G1 and anti-tubulin antibodies and to immunoprecipitation using anti-HA antibody. Immunoprecipitates were subjected to Western blot analysis using an anti-ubiquitin antibody.

**Fig. 3. RILP recruits V1G1 on late endosomal/lysosomal membranes.** **(A)** Post-nuclear supernatants (PNS), cytosol (C) and membrane (M) fractions of control HeLa cells or cells expressing HA-RILP as indicated, treated 3h before harvesting with MG132, were subjected to Western blot analysis using anti-V1G1, anti-HA, anti-V0D1 and anti-GAPDH antibodies. **(B)** Quantification of the amount of V1G1 present in membrane and cytosol normalized for V0D1 and GAPDH, respectively. Histograms represents the average ( $\pm$  s.e.m.) of three independent experiments. **(C)** Lysates of control HeLa cells or cells expressing HA-RILP and V1G1 or just HA-RILP were subjected to immunoprecipitation using mouse anti-HA antibody. Lysates (WB) and immunoprecipitates (IP) were subjected to Western blot analysis using anti-HA, anti-V1G1, anti-V1C1, anti-V0D1 or anti-tubulin specific antibodies.

**Fig. 4. RILP partially colocalizes with V1G1 on late endosomal/lysosomal organelles.** **(A)** HeLa cells transfected with HA-V1G1 (top panel), co-transfected with GFP-RILP and HA-V1G1 (middle panel), or co-transfected with GFP-RILPC33 and HA-V1G1 (bottom panel), were fixed and immunostained for Lamp1 and HA. Bar = 10  $\mu$ m. **(B)** Quantification of the colocalization between Lamp1 and V1G1. Histogram represents the average ( $\pm$  s.e.m.) of three independent experiments where at least 50 cells were quantified per experiment. **(C)** Quantification of the colocalization of V1G1 with GFP-RILP or GFP-RILPC33. Histogram represents the average ( $\pm$  s.e.m.) of three independent experiments where at least 50 cells were

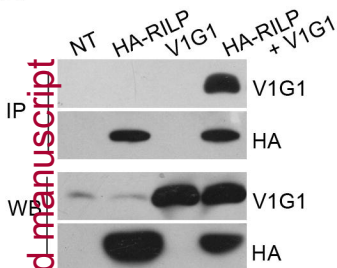
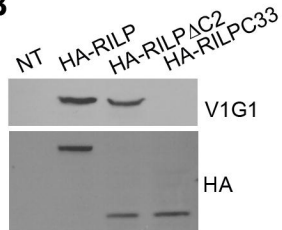
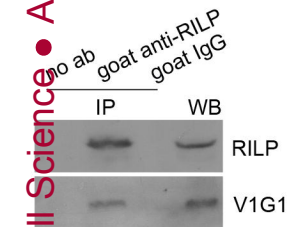
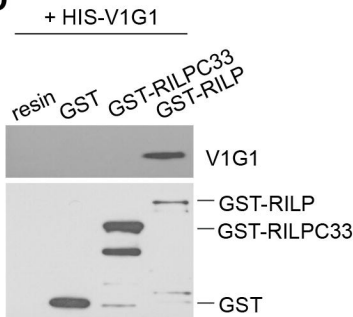
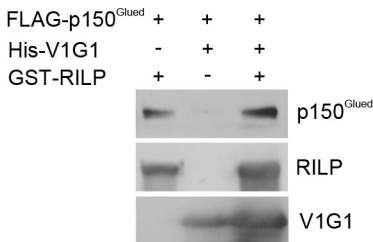
quantified per experiment.

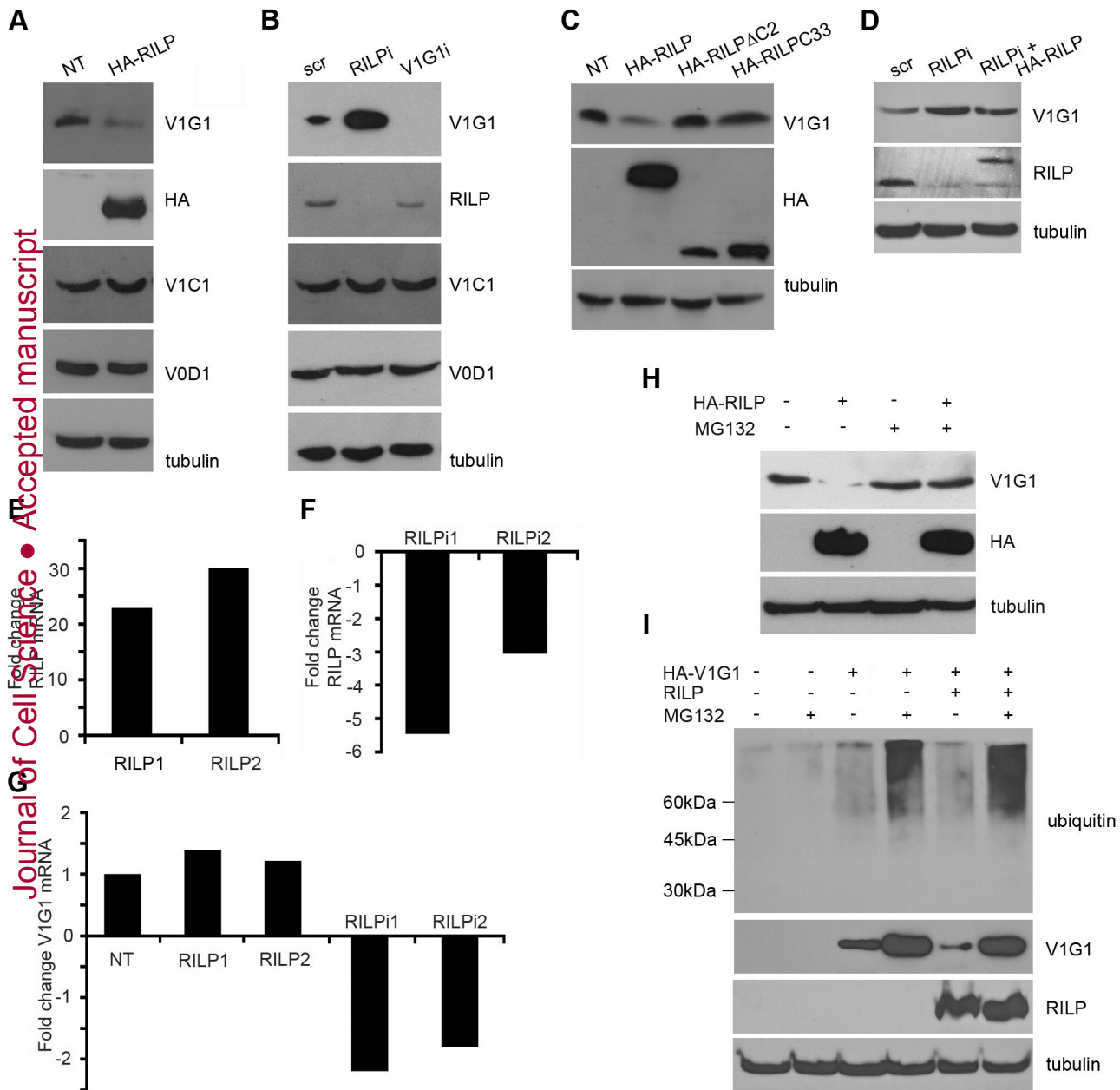
**Fig. 5. RILP depletion affects V1G1 intracellular localization** (A) Control (scr) and RILP-depleted cells (RILPi) were transfected with HA-V1G1, fixed and immunostained for Lamp1, HA and Giantin. Bar = 10  $\mu$ m. (B) Quantification of the colocalization between V1G1 and Lamp1 or V1G1 and Giantin. Histogram represents the average ( $\pm$  standard deviation) of three independent experiments where at least 50 cells were quantified per experiment.

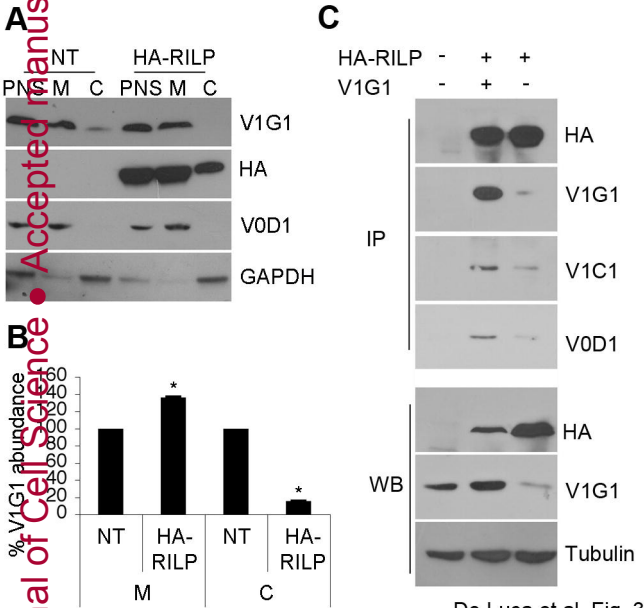
**Fig. 6. Role of Rab7 in the regulation of V1G1.** Lysates of control HeLa cells (NT) or cells expressing HA-Rab7 (A) or of HeLa cells treated with control RNA or Rab7 siRNA (Rab7i) (B) were subjected to Western blot analysis using anti-V1G1, anti-Rab7 and anti-tubulin antibodies. (C) HeLa cells transfected with HA-RILP and HA-Rab7 as indicated were subjected to Western blot analysis using anti-V1G1, anti-HA and anti-tubulin antibodies. (D) Lysates of HeLa cells expressing Myc-Rab7, HA-RILP, HA-RILP $\Delta$ C2, HA-RILPC33 and/or V1G1, as indicated, were immunoprecipitated using mouse anti-V1G1 antibodies. In one sample RILP was also silenced (RILPi) before expression of Myc-Rab7 and V1G1 (lane 6). Immunoprecipitates were subjected to Western blot analysis using rabbit anti-Myc, rabbit anti-HA and chicken anti-V1G1 antibodies.

**Fig. 7. RILP and V1G1 control V-ATPase activity.** (A) HeLa cells treated with control RNA (scr) or RILP siRNA (RILPi) were incubated with LysoTracker Red for 30 min and analyzed by live microscopy. (B) The LysoTracker Red intensity, relative to scr, was quantified. Histogram represents the average ( $\pm$  standard deviation) of three independent experiments where at least 50 cells were quantified per experiment. (C) Lysates of control HeLa cells (NT) or cells treated with Bafilomycin A1 or cells expressing transiently or stably (clones 1 and 2) HA-V1G1, or expressing transiently or stably (clones 1 and 2) sh-V1G1 or control RNA (sh-C) were subjected to Western blot analysis using anti-cathepsin D and anti-tubulin antibodies. (D) Quantification of cathepsin D forms. Histogram represents the average ( $\pm$  s.e.m.) of three independent experiments.

**Fig. 8. Proposed model for the functional interactions between RILP, V1G1 and Rab7.** RILP strictly regulates V1G1 abundance and localization promoting activation of the proton pump on late endosomes/lysosomes. The binding of RILP to Rab7 induces V1G1 recruitment on late endosomal/lysosomal membranes and, in turn, promotes assembly of the pump on these membranes. In addition the ratio between RILP and Rab7 is fundamental for V1G1 protein abundance; an excess of RILP unbound to Rab7 (as in the case of RILP overexpression or of Rab7 silencing) leads to V1G1 ubiquitination and degradation via a proteasome–dependent mechanism.

**A****B****C****D****E**





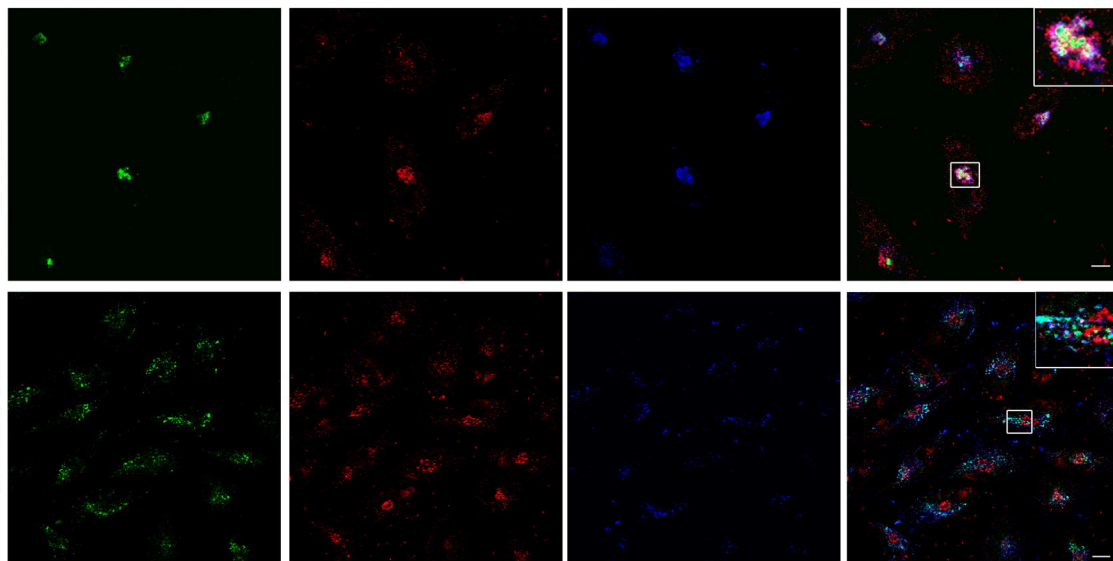
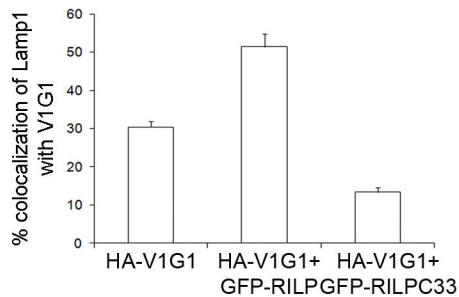
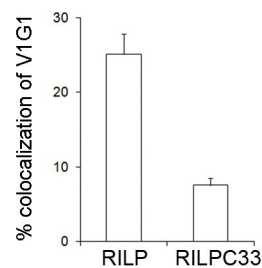


**A**

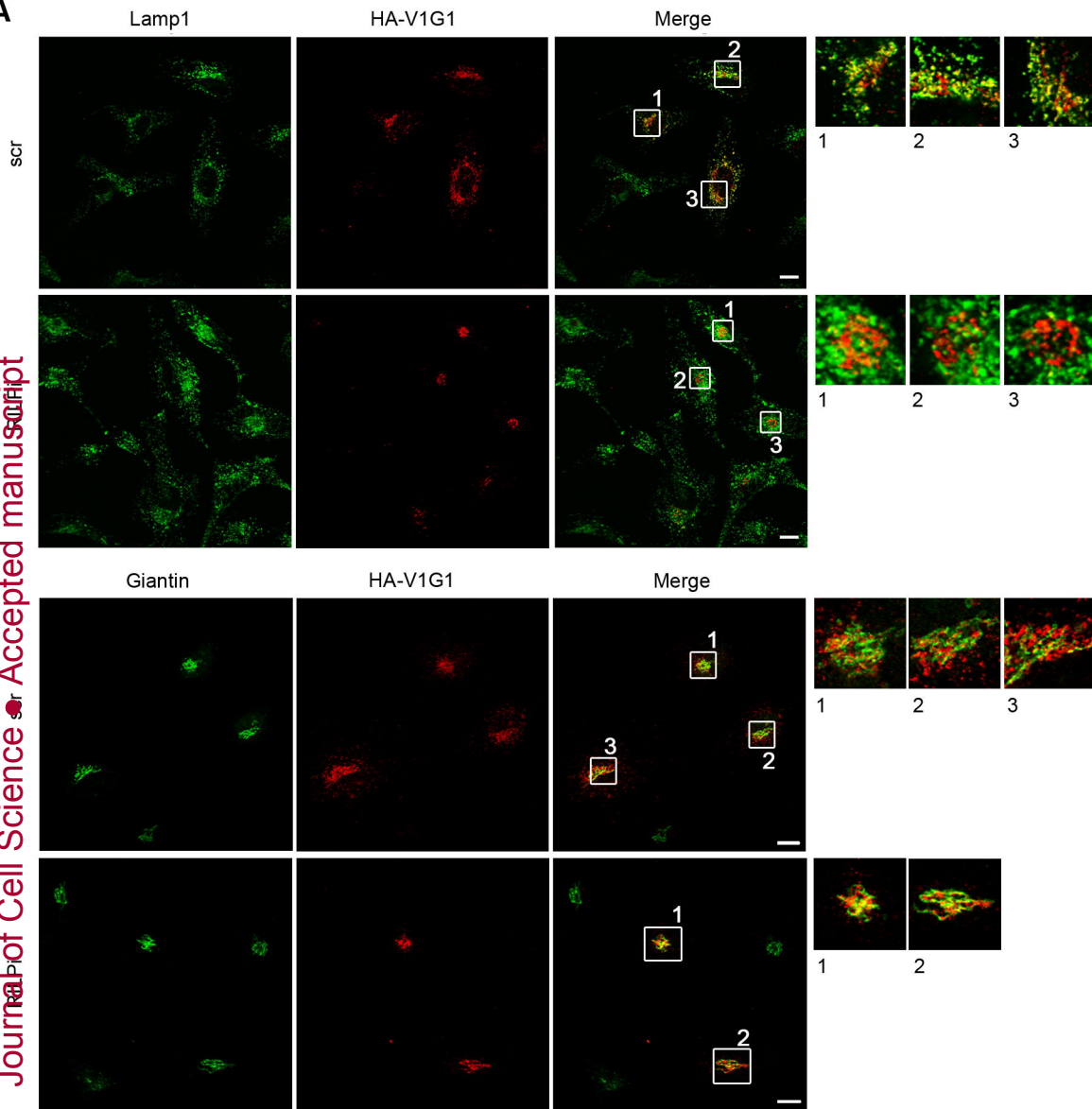
HA-V1G1

Lamp1

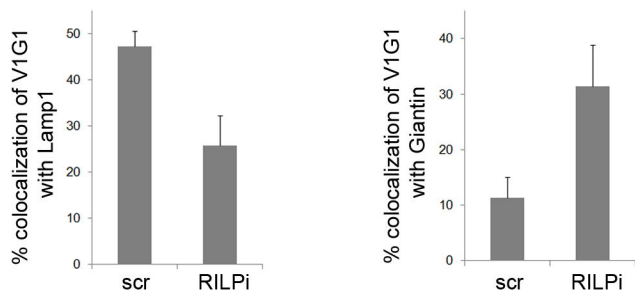
Merge

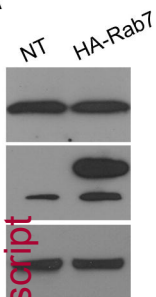
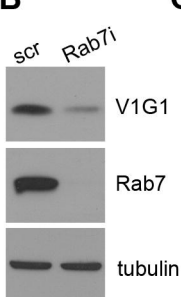
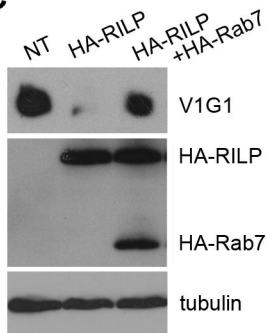
**B****C**

**A**



**B**



**A****B****C****D**